

CFD Analysis of Whale Inspired Hydrofoil with Different Angles of Attack

Mr. K.Joseph*, Mr. V.Pradeep*, Mr. K. Dileep kumar*, Mr. B.Nikhil Varma*, Mr. C.Naveen Sapthagiri*, Ms. M Amrutha**, Mr. DJ Johnson**

*UG students, **Faculty, Department of Mechanical Engineering College, Pragati Engineering College (A)

ABSTRACT - Recent discoveries in the biomimicry field found that mimicking Humpback whale flippers can give us better Drag and Lift coefficients. CFD analysis is done on whale inspired modified NACA-0021 foil with sinusoidal leading edge. And Velocity and pressure contours are generated to see the results. It has found that with the change in the angle of attack of each foil the velocity contour changes. The geometry was managed using the Design Modeler tool. The fluid flow simulation was carried out using ANSYS Fluent. The result showed the performance of E387 is better than other hydrofoils as it gives better lift force with the least drag force, resulting in better hydrodynamics of turbine blade. Overall, the value of lift and drag coefficients at 10° was more consistent than 0° and 20° AOA.

Key words: CFD, Hydrofoil, Angles, AOA, Ansys, E387

I. INTRODUCTION

It is a fact of common experience that a body in motion through a fluid experiences

a resultant force which, in most cases is mainly a resistance to the motion. A class of body exists, however, for which the component of the resultant force normal to the direction to the motion is many times greater than the component resisting the motion, and the possibility of the movement of fast ships above water depends on the use of the body of this class for wing structure. Hydrofoil is such an aerodynamic shape that when it moves through water, the water is split and passes above and below the wing. The wing's upper surface is shaped so the water rushing over the top speeds up and stretches out. This decreases the water pressure above the wing. The water flowing below the wing moves in a comparatively straighter line, so its speed and water pressure remain the same. Since high water pressure always moves toward low water pressure, the water below the wing pushes upward toward the water above the wing. The wing is in the middle, and the whole wing is "lifted." The faster a fast boat moves, the more lift there is. And when the force of lift is greater than the force of gravity, the fast boat is able to lift above water. AOA is the angle between the oncoming water or relative wind and a reference line on the fast boat or wing. Sometimes the reference line is a line connecting the leading edge and trailing edge at some average point on a wing. So in this report I have basically taken a hydrofoil NACA 0021 and with various angles of attacks and keeping velocity constant I concluded a result on maximum lift and drag coefficient. Surfing is a global sport that involves catching and riding

waves on a surfboard fitted with fins. Currently, only one other study compares field performance and numerical (computational fluid dynamics, CFD) results of different surfboard fin designs [1]. The study involved a single, longboard-style surfing fin, comparing a standard longboard fin to a tubercled, "real whale" (RW) design. Static CFD results showing improved efficiency and an expanded operating envelope for RW led to field testing of a prototype RW design. Results from over 650 surfed waves, comparing RW to a standard longboard fin confirmed the CFD results, with significant improvements in max speed, average speed, and distance surfed on individual waves. Rather than single longboard fins, the present study compares field and numerical results from 3-fin thruster sets. Introduced by Simon Anderson in 1980 [2], thruster sets are commonly used in high performance shortboard surfing, where maneuverability and control are key performance factors. Specifically, this paper focuses on the cutback, or top turn (Figure S1), an important maneuver during recreational and competitive surfing [3–5]. To gain more understanding of field performance of RW vs. control fins attached to shortboards, this study uses dynamic CFD to simulate field results and compare forces imparted to 3-fin thruster sets.

1.1 OBJECTIVE

1. To check the behavior of CL (coefficient of Lift), CD (coefficient of Drag) in
2. NACA- 0012 (National Advisory Committee for Aeronautics) When the velocity is kept constant. When the AOA (Angle Of Attack) is varied from -25° to 25° with a gap of 5 degrees.

3. To compare the obtained CD and CL with corresponding baseline NACA 0012 foil.
4. To determine different velocity contours and Pressure fields on the surface of foil.

1.2 METHODOLOGY

1. Computational Fluid Dynamics analysis of hydrofoil system is done in ANSYS workbench to see overall effect on velocity distribution and CL, CD is calculated.
2. Velocity is assumed to be 2.1415 m/s 11 cases are taken:
3. Where the AOA is $-25^\circ, -20^\circ, -15^\circ, -10^\circ, -5^\circ, 0^\circ, 5^\circ, 10^\circ, 15^\circ, 20^\circ, 25^\circ$.
4. Lift coefficient and drag coefficient is calculated for each possibility.
5. Tabular and Graphical presentation are obtained using MS Excel.

Flow behaviour of a hydrofoil with leading-edge tubercles was experimentally studied using particle image velocimetry technique at a Reynolds number of $Re = 1.4 \times 10^4$. Four angles-of-attack of $\alpha = 0^\circ, 10^\circ, 15^\circ$ and 20° were considered. Proper orthogonal decomposition (POD) technique was used to analyse the instantaneous velocity fields and derive information on the variation of corresponding coefficients and flow energy content. Results show that tubercles can alter the vortical behaviour and lead to increased flow unsteadiness. At lower angles-of-attack, the flow behaviour for the baseline hydrofoil is dominated by wake vortex-shedding, which represents a significant percentage of flow energy content. In contrast, separated shear layer and flow reattachment become the dominant flow behaviour for the hydrofoil with tubercles. Higher order POD modes 4 and 5 are associated with coherent vortex convection in the shear layer, which is similar to that of the baseline hydrofoil at higher angles-of-attack. At $\alpha = 15^\circ$, POD modes 2 and 3 along the tubercle trough and peak show coherent vortex-shedding in the flow separation region. However, unstable flow separations are observed along the Mid-plane between the peaks and troughs, as a result of the separated shear layers associated with POD modes 1 and 2. In this report, the hydrodynamic performance of a NACA 634-021 (baseline) foil and two modified foils with leading-edge protuberances was numerically investigated using the Spalart-Allmaras turbulence model. It was found that modified foils performed worse than the baseline foil at pre-stall angles, while the lift coefficients at high angles of attack of the modified foils were increased. Both the deterioration of pre-stall and the improvement of post-stall performance were enhanced with larger amplitude of protuberance. Near-wall flow visualizations showed that the leading-edge protuberances worked in pairs at high angles of attack, producing different forms of streamwise vortices. An attached flow along some valley sections was observed, leading to a higher local lift coefficient at post-stall angles. Most experimental and numerical investigations carried out for low Reynolds number conditions have related the

relative improvements observed poststall to “bi-periodic” flow structures, developing over tubercles pairs. In this study, a numerical approach is employed to show the emergence of higher-order patterns in the flow over a stalling NACA 0021 hydrofoil with sinusoidal leading edge. The effect of the number of sinusoidal tubercles defining the leading edge of the hydrofoil model on the prediction of “bi-periodic” or “tri-periodic” flow structures is particularly analyzed to interpret the uncertainty found on the resulting hydrodynamic performance.

Lift and drag:

Lift and Drag Lift on a body is defined as the force on the body in a direction normal to the flow direction. Lift will only be present if the fluid incorporates a circulatory flow about the body such as that which exists about a spinning cylinder. The velocity above the body is increased and so the static pressure is reduced. The velocity beneath is slowed down, giving an increase in static pressure. So, there is a normal force upwards called the lift force. The drag on a body in an oncoming flow is defined as the force on the body in a direction parallel to the flow direction. For a windmill to operate efficiently the lift force should be high and drag force should be low. For small angles of attack, lift force is high and drag force is low. If the angles of attack (α) increase beyond a certain value, the lift force decreases and the drag force increases. So, the angle of attack plays a vital role.

II. METHODOLOGY

CFD analysis on whale inspired hydrofoil for different Angle of Attacks:

Airfoil Design: NACA- 0012(National Advisory Committee for Aeronautics)

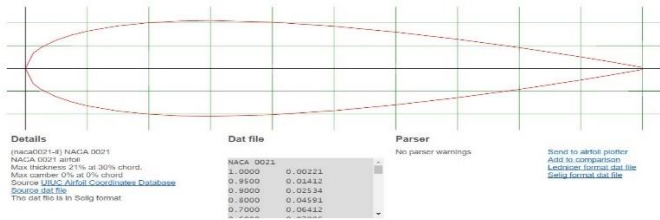
Angle of Attacks: $-25^\circ, -20^\circ, -15^\circ, -10^\circ, -5^\circ, 0^\circ, 5^\circ, 10^\circ, 15^\circ, 20^\circ, 25^\circ$.

- Analysis: Lift coefficients, Drag coefficients, and Velocity contour on the x-y plane perpendicular to max amplitude.
- Amplitude: 10% of Chord Length.
- Wavelength: 50% of chordlength

4.1 Method of Analysis

The hydrofoil NACA 0021 is chosen for blade modeling. NACA 0021 profiles are obtained from Design Foil Workshop for various chords. The modeling is done with Solid Works. The blade is generated for the specification.

NACA 0021 (naca0021-il)
NACA 0021 - NACA 0021 airfoil



Construction of Hydrofoil

4.2 Theoretical Calculation

The angle of attack value is given as input in the Design Foil Workshop software and the values of both the coefficients are found out. The lift and drag forces are calculated by the following formula and the lift to drag ratio (L/D ratio) is also found out.

$$\text{Lift} = (1/2) * \rho * C_L * c * L * V_{rel}^2$$

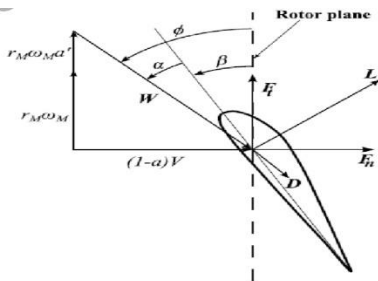
$$\text{Drag} = (1/2) * \rho * C_D * c * L * V_{rel}^2$$

Where ρ - density of air - 1.225 kg/m³

c - Chord length in meter - 1m

L - Length of the blade element - 1m

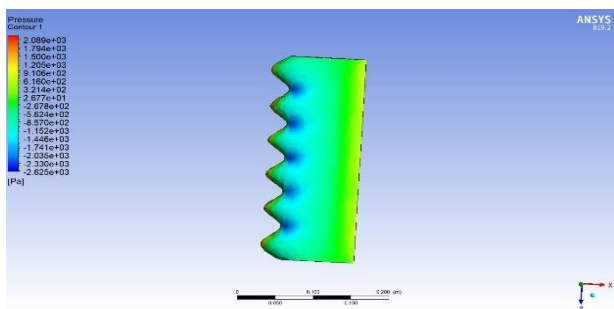
$$V_{rel} - \text{relative velocity of air in m/s} = ((V_0)^2 + (\omega r)^2)^{0.5}$$



Po Stagnation Pressure [Pa] or [lbf/ft²]

P Pressure [Pa] or [lbf/ft²]

6.1 For Angle of Attack 0 degrees



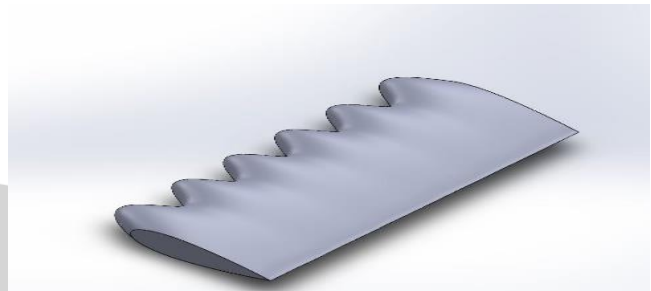
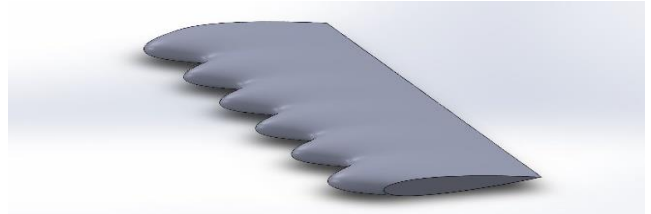
Pressure Countour on hydrofoil

Pressure contour for NACA 0021 at AOA 5 degrees and velocity= 2.1516m/s

- r Density [kg/m³] or [lbf/ft³]
- V Velocity [m/s] or [ft/s]
- g Gravitational Constant [m/s²] or [ft/s²]
- y Height [m] or [ft]

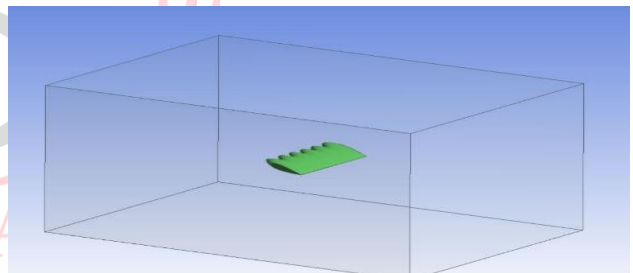
III. CAD MODELLING

5.1 Hydrofoil NACA - 0021



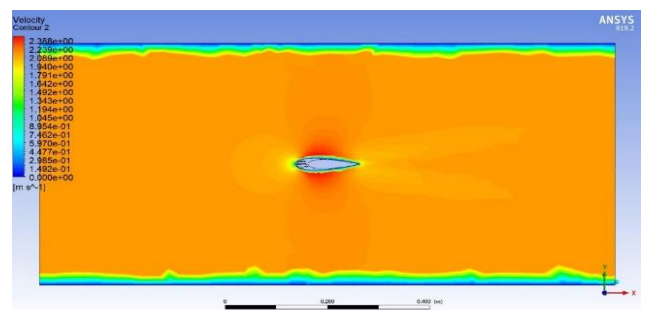
5.1: CAD model of Hydrofoil

5.2 Final CAD Model



5.2 CAD model of enclosed figure around an hydrofoil.

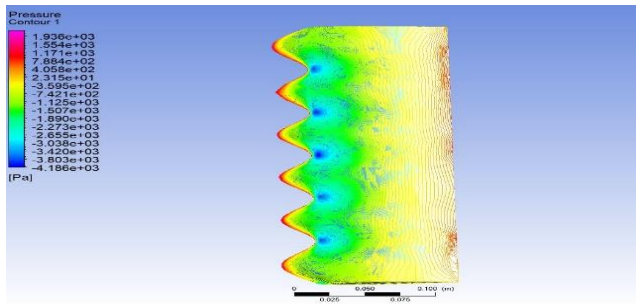
IV. RESULTS AND DISCUSSION



Velocity Contour on 1 plane with max amplitude Velocity contour for NACA 0021 at AOA 0 degrees and velocity= 2.1516m/s.

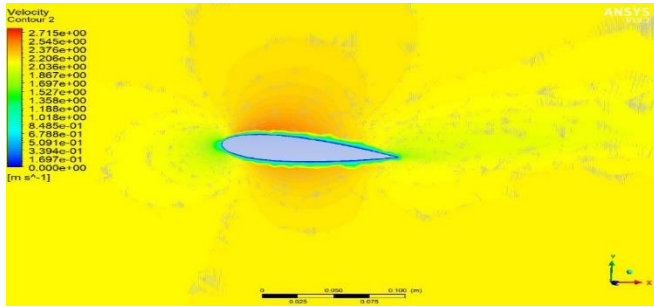
6.2 For Angle of Attack 5 degrees

Pressure Countour on hydrofoil



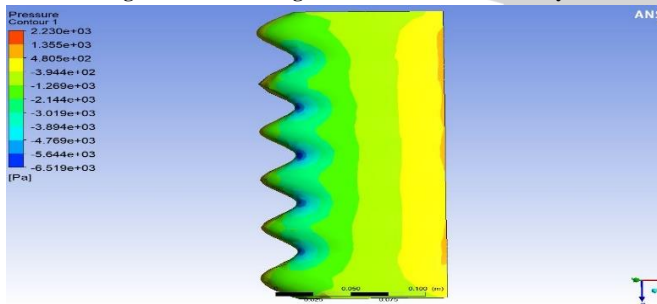
Pressure contour for NACA 0021 at AOA 5 degrees and velocity= 2.1516m/s

Velocity Contour on \perp plane with max amplitude



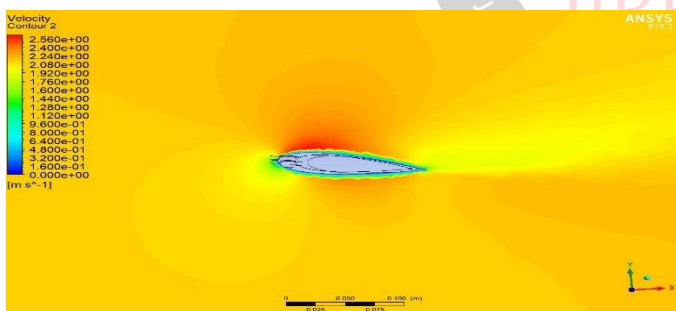
Velocity contour for NACA 0021 at AOA 5 degrees and velocity= 2.1516m/s.

6.3 For Angle of Attack 10 degree Pressure Countour on hydrofoil



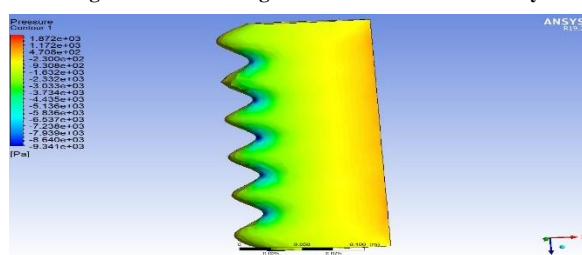
Pressure contour for NACA 0021 at AOA 10 degrees and velocity= 2.1516m/s

Velocity Contour on \perp plane with max amplitude



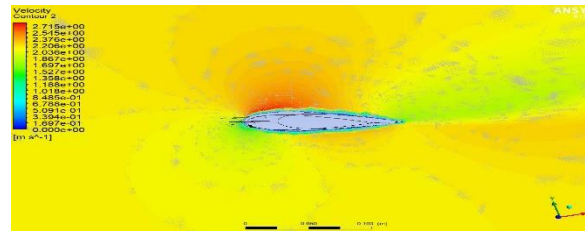
Velocity contour for NACA 0021 at AOA 10 degrees and velocity= 2.1516 m/s.

6.4 For Angle of Attack 15 degrees Pressure Countour on hydrofoil



Pressure contour for NACA 0021 at AOA 15 degrees and velocity= 2.1516m/s

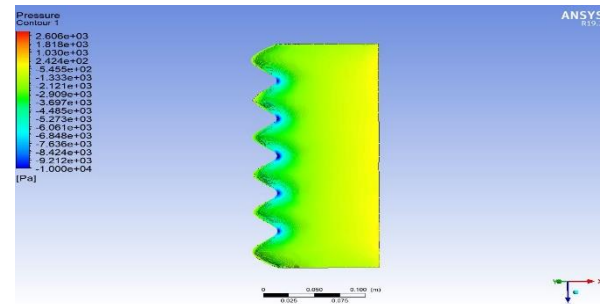
Velocity Contour on \perp plane with max amplitude



Velocity contour for NACA 0021 at AOA 15 degrees and velocity= 2.1516 m/s.

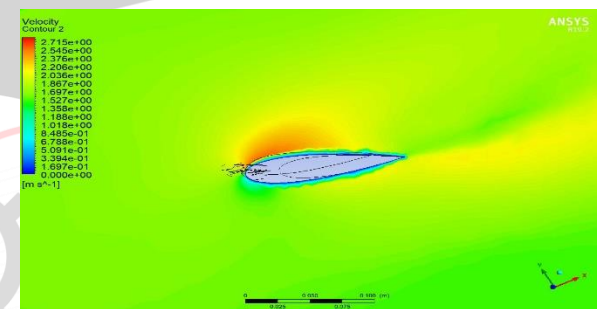
6.5 For Angle of Attack 20 degrees

Pressure Countour on hydrofoil



Pressure contour for NACA 0021 at AOA 20 degrees and velocity= 2.1516m/s

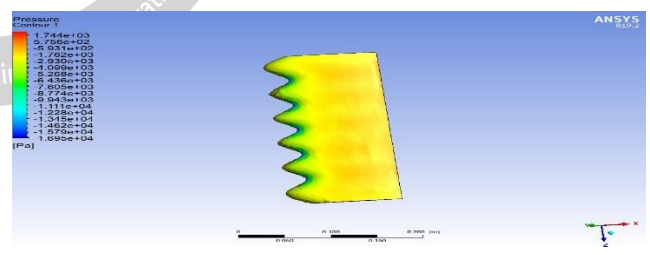
Velocity Contour on \perp plane with max amplitude



Velocity contour for NACA 0021 at AOA 20 degrees and velocity= 2.1516 m/s

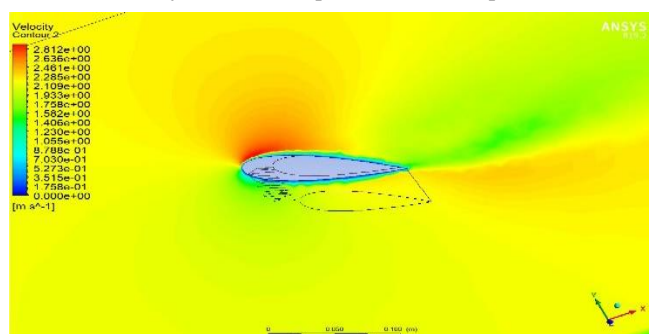
6.6 For Angle of Attack 25 degrees

Pressure Countour on hydrofoil



Pressure contour for NACA 0021 at AOA 25 degrees and velocity= 2.1516m/s

Velocity Contour on \perp plane with max amplitude

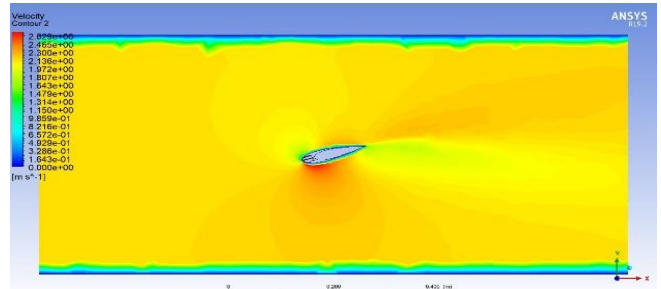
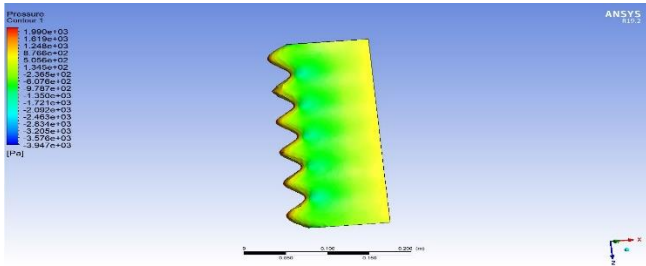


Velocity contour for NACA 0021 at AOA 25 degrees and velocity= 2.1516 m/s.

Pressure contour for NACA 0021 at AOA -15 degrees and velocity= 2.1516m/s

6.7 For Angle of Attack -5 degrees Pressure Countour on hydrofoil

Velocity Contour on \perp plane with max amplitude

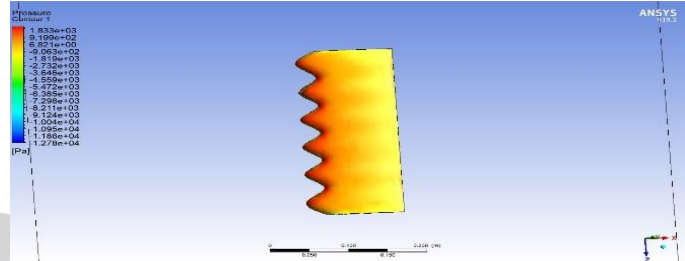
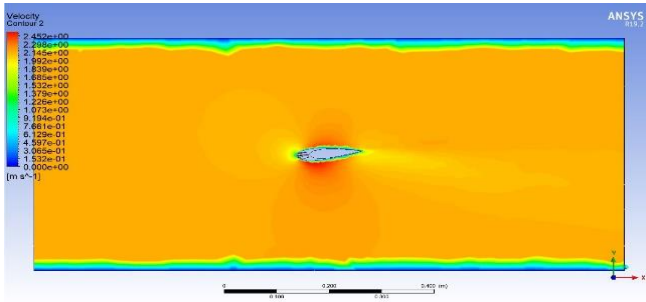


Pressure contour for NACA 0021 at AOA -5 degrees and velocity= 2.1516m/s

Velocity contour for NACA 0021 at AOA -15 degrees and velocity= 2.1516 m/s

Velocity Contour on \perp plane with max amplitude4

6.10 For Angle of Attack -20 degrees Pressure Countour on hydrofoil

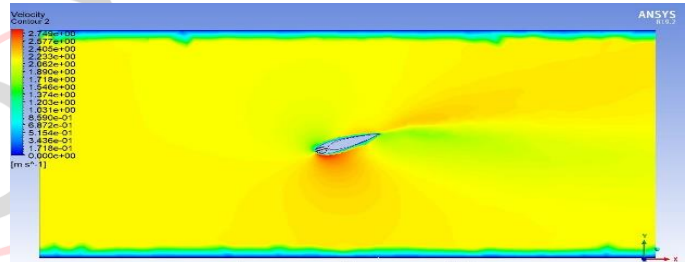
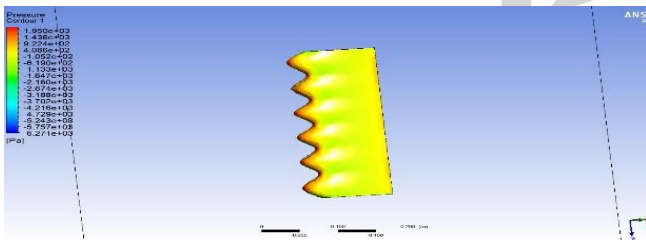


Velocity contour for NACA 0021 at AOA -5 degrees and velocity= 2.1516 m/s

Pressure contour for NACA 0021 at AOA -20 degrees and velocity= 2.1516m/s

6.8 For Angle of Attack -10 degree Pressure Countour on hydrofoil

Velocity Contour on \perp plane with max amplitude

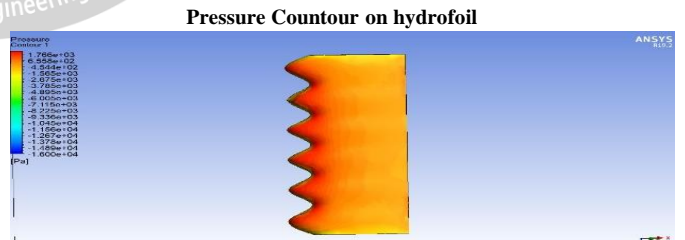
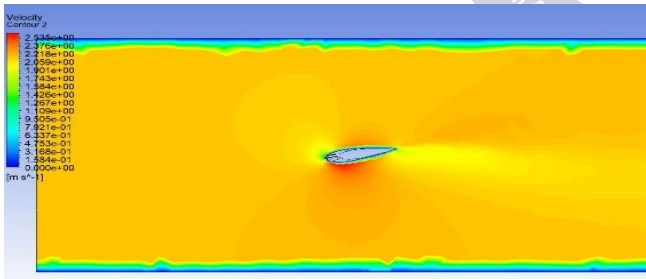


Pressure contour for NACA 0021 at AOA -10 degrees and velocity= 2.1516m/s

Velocity contour for NACA 0021 at AOA -20 degrees and velocity= 2.1516 m/s.

Velocity Contour on \perp plane with max amplitude

6.11 For Angle of Attack -25 degrees

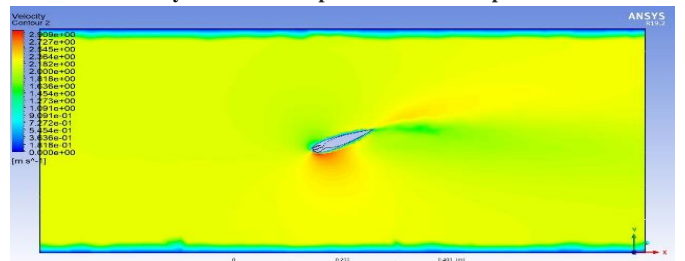
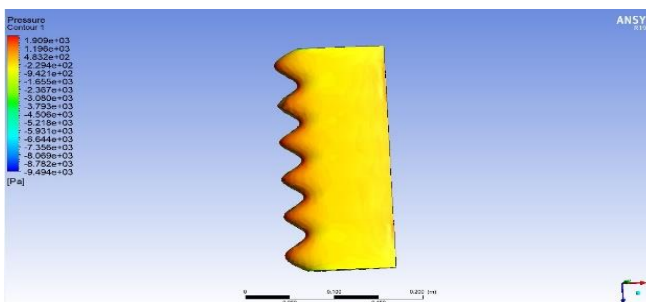


Velocity contour for NACA 0021 at AOA -10 degrees and velocity= 2.1516 m/s

Pressure contour for NACA 0021 at AOA -25 degrees and velocity= 2.1516m/s

6.9 For Angle of Attack -15 degrees Pressure Countour on hydrofoil

Velocity Contour on \perp plane with max amplitude



Velocity contour for NACA 0021 at AOA -25 degrees and velocity= 2.1516 m/s.

Velocity contour for NACA 0021 at AOA -25 degrees and velocity= 2.1516 m/s.

V. CONCLUSION

- CAD model of NACA 0012 hydrofoil is generated in solid works
- Hydrofoil is modified with Sinusoidal Leading Edge and imported to ansys workbench19.2
- Simulations are carried out with constant velocity of 2.1516 m/s with different angle of attack.
- Hence it is considered that both hydrofoils are moderated in either performance as for NACA4412 this type of hydrofoils gives a higher lift force and low drag force .
- When we used angle 10 o the Drag force is decreased and Lift force is increased
- At 10o angle the coefficient of drag is produced 4.5910086 and coefficient of lift is produced 36.368574

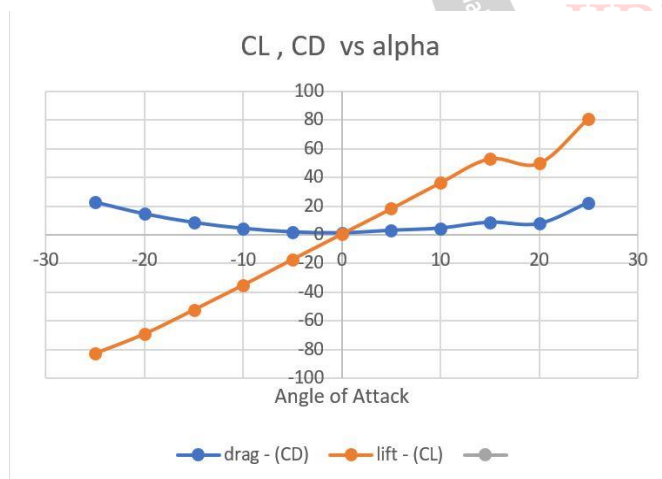
7.1 Tabulated data:

- The L & D/alpha with constant velocity is plotted in Fig. below. The correlation between coefficient of lift and drag with Angle of Attack is shown in.

Angle of Attack	drag - (CD)	lift - (CL)
-25	22.78093	-82.43806
-20	14.56748	-68.87283
-15	8.52981	-52.11647
-10	4.37829	-34.87152
-5	1.92317	-16.99543
0	1.23984	0.67219
5	3.0587232	18.22219
10	4.5910086	36.368574
15	8.7247219	53.113524
20	7.7375673	49.875415
25	22.428539	81.007318

L & D/α RATIO AT VARIOUS ANGLE OF ATTACKS AT CONSTANT VELOCITY

7.2 Graphical Representation:



L&D VS ANGLE OF ATTACK WITH CONSTANT VELOCITIES

VI. REFERENCE

- [1] Cai, C., Zou, Z. Liu, S., and Wu, Y. (2015). Numerical investigations of hydrodynamic performance of hydrofoils with leading-edge protuberances. *Advances in Mechanical Engineering* 7(7) Article number 1687814015592088
- [2] Charalambous, N. and Eames, I. (2017). A detail computational hydro – acoustics analysis for hydrofoils with straight and wavy leading edges. *Fifth International Symposium on Marine Propulsion, SMP'17, Espoo, Finland, June 2017*
- [3] Custodio D, Henoch C, Johari H. 2018. Cavitation on hydrofoils with leading edge protuberances. *Ocean Engineering* 162: 196-208
- [4] Custodio D, Henoch C, Johari H. 2018. Cavitation on hydrofoils with leading edge protuberances. *Ocean Engineering* 162: 196-208
- [5] Wei, Z., New, T. H. and Cui, Y. D. 2015. An experimental study on flow separation control of hydrofoils with leading-edge tubercles at low Reynolds number. *Ocean Engineering* 108:336-349
- [6] Wei, Z., Zang, B., New, T.H. and Cui, Y.D., 2016. A proper orthogonal decomposition study on the unsteady flow behaviour of a hydrofoil with leading-edge tubercles. *Ocean Engineering*, 121, 356-368.
- [7] I. Nachtane, M.; Tarfaoui, M.; Goda, I.; Rouway, M. A review on the technologies, design considerations and numerical models of tidal current turbines. *Renew. Energy* 2020, 157, 1274–1288. [CrossRef]
- [8] Xu, W.; Xu, G.; Duan, W.; Song, Z.; Lei, J. Experimental and numerical study of a hydrokinetic turbine based on tandem flapping hydrofoils. *Energy* 2019, 174, 375–385. [CrossRef] *Processes* 2021, 9, 1656 11 of 11
- [9] Hao, W.; Li, C. Performance improvement of adaptive flap on flow separation control and its effect on VAWT. *Energy* 2020, 213, 118809. [CrossRef]
- [10] Yan, H.; Su, X.; Zhang, H.; Hang, J.; Zhou, L.; Liu, Z.; Wang, Z. Design approach and hydrodynamic characteristics of a novel bionic airfoil. *Ocean Eng.* 2020, 216, 108076. [CrossRef]
- [11] Velte, C.M.; Hansen, M. Investigation of flow behind vortex generators by stereo particle image velocimetry on a thick airfoil near stall. *Wind Energy* 2013, 16, 775–785. [CrossRef]
- [12] Hussain, S.; Liu, J.; Wang, L.; Sundén, B. Suppression of endwall heat transfer in the junction region with a symmetric airfoil by a vortex generator pair. *Int. J. Therm. Sci.* 2019, 136, 135–147. [CrossRef]
- [13] Itsariyapinyo, P.; Sharma, R.N. Large Eddy simulation of a NACA0015 circulation control airfoil using synthetic jets. *Aerosp. Sci. Technol.* 2018, 82–83, 545–556. [CrossRef]
- [14] Tousi, N.M.; Coma, M.; Bergadà, J.M.; Pons-Prats, J.; Mellibovsky, F.; Bugeda, G. Active Flow Control Optimisation on SD7003 Airfoil at Pre and Post-stall Angles of Attack using Synthetic Jets. *Appl. Math. Model.* 2021, 98, 435–464. [CrossRef]